



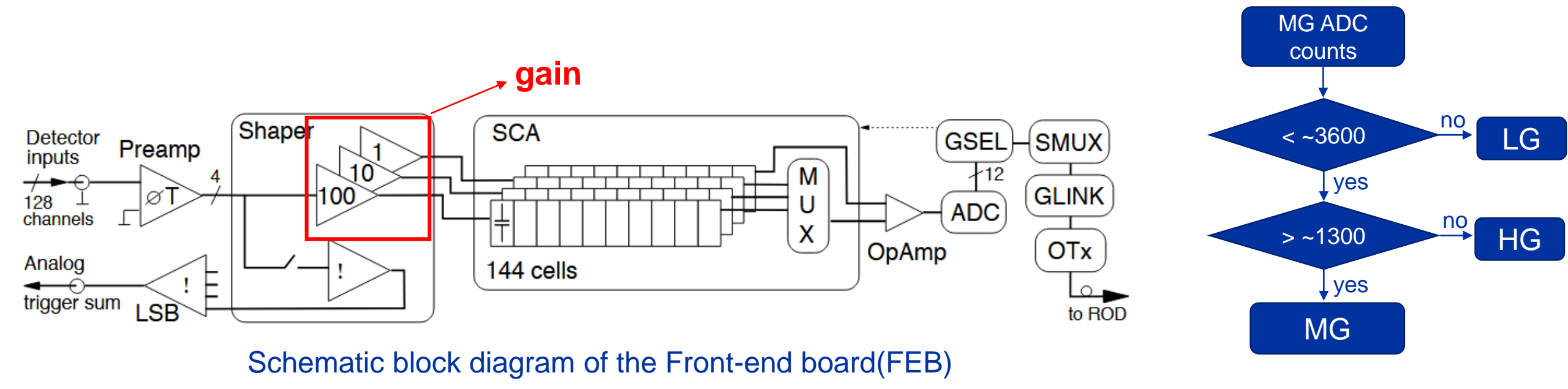
# Run3 L2Gain Intercalibration in the ATLAS Experiment

Zijiang Wang
IHEP CAS
CLHCP 2025, Xinxiang

2025.11.01

#### **Introduction – Gain**

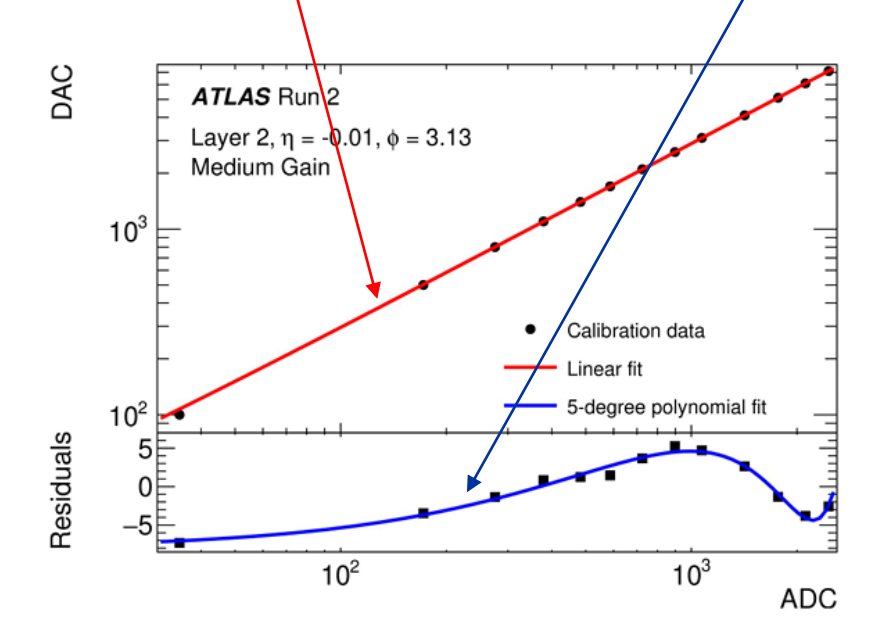
- Data comes from detectors and further amplified by shaper chips to produce three linear gain scales
  - ➤ 1 for low gain (LG)
  - > 9.9 for medium gain (MG)
  - > 93 for high gain (HG)
- The Gain Selector chips (GSEL) choose one of the three gains to use, based on the value of the peak sample in the medium gain compared to two reference thresholds.

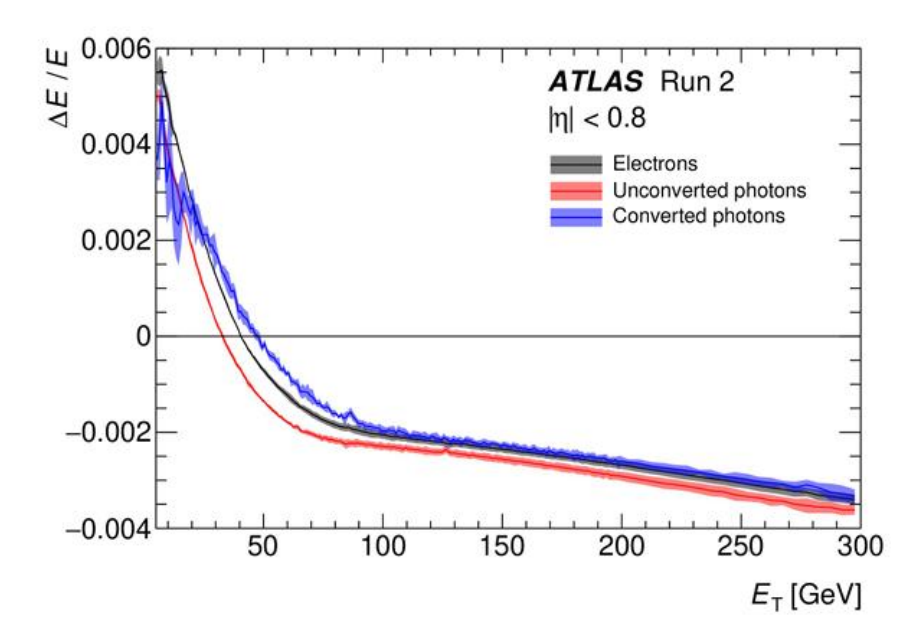


#### Introduction – ADC non-linearity correction

#### • Energy reconstruction in LAr calorimeter

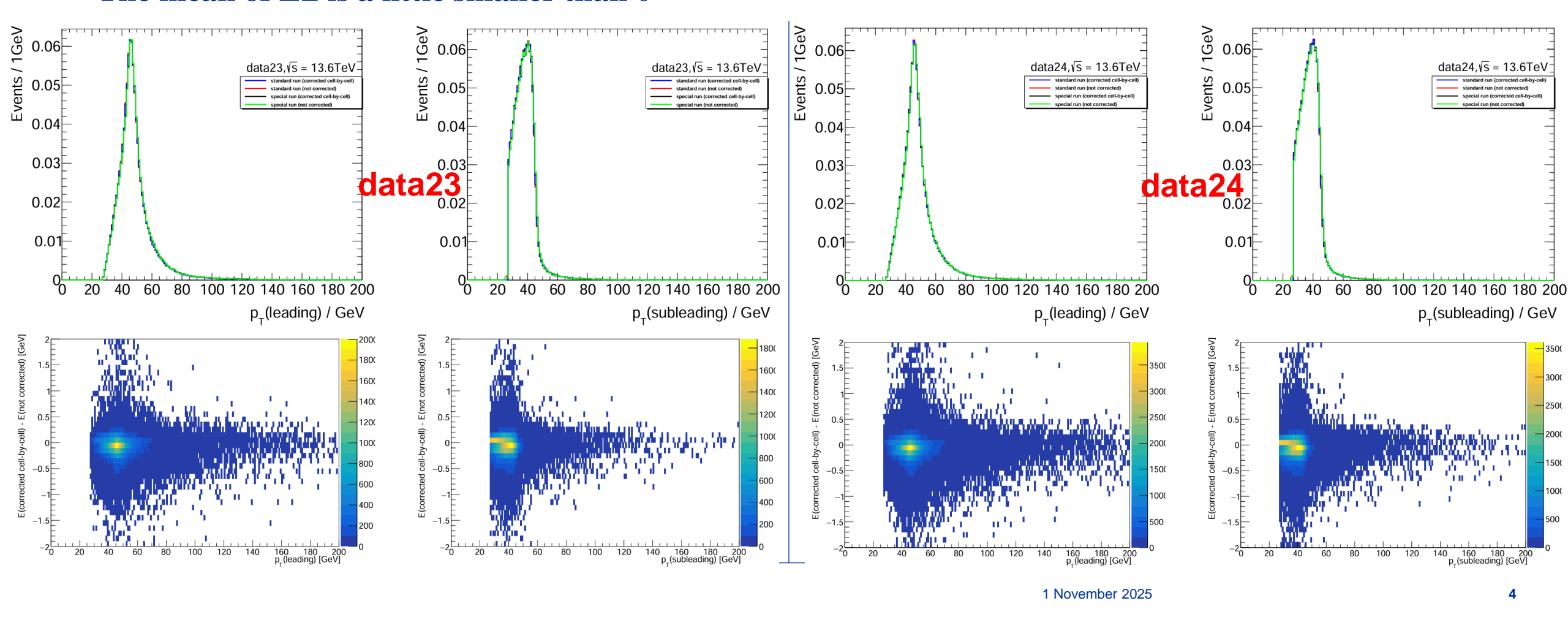
- ➤ A linear conversion from ADC (analog-to-digital converter) counts to current
- ➤ A linear factor converting into energy
  - The fit to calibration show non-zero residual w.r.t. injected current (i.e. DAC) and needs to be corrected
- $\triangleright$  Cluster energies are increased by about 0.4% at low  $E_T$ , and decreased by about 0.2% at high  $E_T$





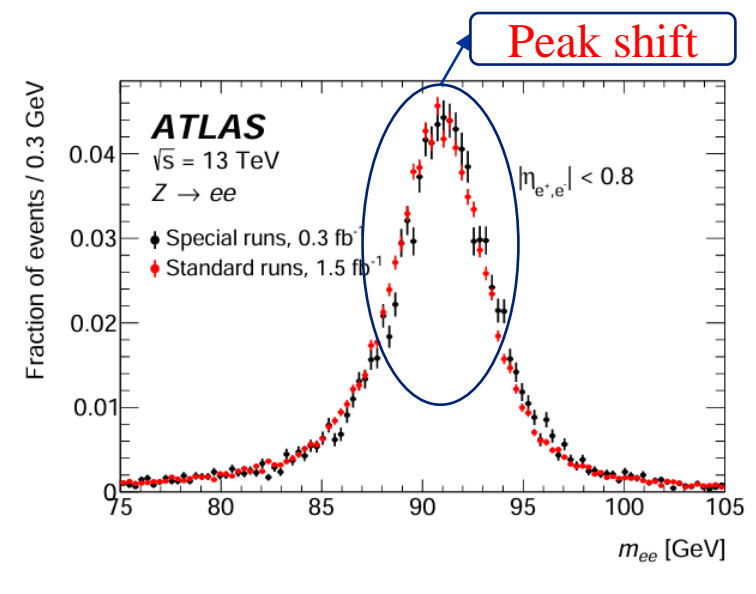
#### $p_T$ distributions for data23 and data24

- The distributions of  $p_T$  and  $(E(corr) E(not\ corr)\ vs\ p_T)$  are shown for leading and subleading electrons.
- The mean of  $\Delta E$  is a little smaller than 0



#### **Motivation**

- $Z \rightarrow e^+e^-$  channel is used for Egamma calibration
  - $\triangleright$  Standard configuration: the high gain readout is used for the majority of cells in clusters of electrons in  $Z \rightarrow ee$
  - $\succ$  the transition to medium gain: ~25GeV/cell in 2<sup>nd</sup> layer for  $|\eta| < 0.8$ , corresponding to electrons of  $E_T = 50 \sim 60$ GeV
- Use special runs to intercalibration High Gain(HG) and Medium Gain(MG)
  - $\triangleright$  In Run2, there is a noticeable shift of the peak in  $m_{ee}$  distribution between HG and MG
  - The threshold to switch from HG to MG readout for the cells in the second layer was lowered for special runs so that the MG readout is used for majority of cells



#### **Event selection**

• After MG and HG ADC correction, we calibrate MG and HG response using  $Z \rightarrow ee$  mass peaks

- The model used for Run3 datasets
  - ►ESModel: es2022\_R22\_PRE
  - ➤ Geometry: ATLAS-R3S-2021-03-02-00
  - ➤ MVAfolder = "egammaMVACalib/offline/v7 pre"
- In event level:
  - ➤ Pass trigger: HLT\_2e24\_lhvloose\_L12EM20VH for data23 HLT\_2e24\_lhvloose\_L12eEM24L for data24
  - $> n_e \ge 2$
  - $\rightarrow$  ( $P_t > 27$ GeV & pass Medium ID &  $|\eta| < 2.47$ ) for leading and subleading e
  - $\triangleright$  Exclude  $\eta_{calo}[-0.05, 0.45]$  and  $\phi_{calo}[0.88, 1.25]$  for leading and subleading e

Excluded due to FEB issue in Run2 special runs,

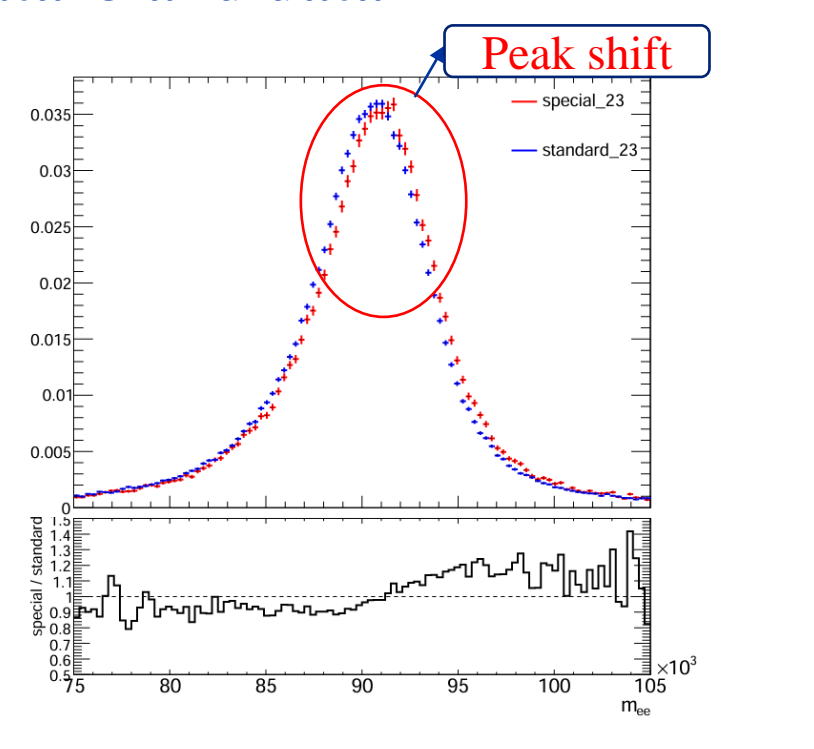
1 November 2025

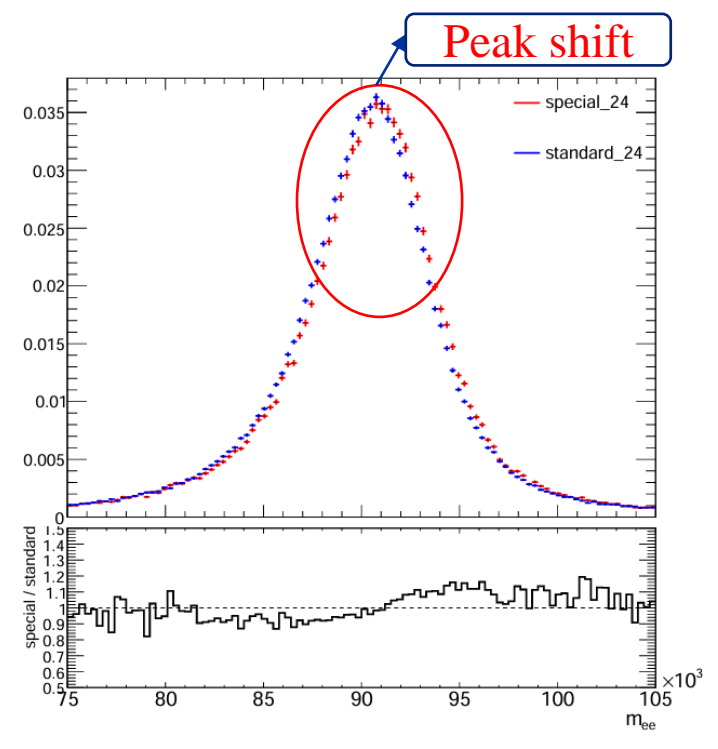
No layer, in-situ scales applied
 same for Run3 here to compare with Run2 result.
 FEB issue is fixed in Run3, will keep these events in

MVA calibrated energy is being compared between special and standard runs

## $m_{ee}$ distribution comparison

• Disagreement between  $M_{ee}$  obtained from HG readout and MG readout is obvious both in data23 and data24





 $m_{ee}$  distribution comparison between standard run and special run for data23 and data24

#### Lineshape method

#### • Approach used to obtain the energy scale $(\alpha)$

- $\triangleright$  Categorize  $m_{ee}$  into 25 bins, 5 bins of  $|\eta_{e1}| \times 5$  bins of  $|\eta_{e2}|$ 
  - $|\eta|$  bins:[0, 0.8), [0.8, 1.37), [1.37, 1.5), [1.5, 1.8), [1.8, 2.47]
  - Obtain the  $m_{ee}$  distribution in each category
- $\triangleright$  Fit  $m_{ee}$  histograms of standard run
  - Fit the histograms with three Gaussian function and get mean( $\mu_{std}$ ) and sigma( $\sigma_{std}$ ) of these functions
  - Build based-on standard run three Gaussian function to described  $m_{ee}$  of special run

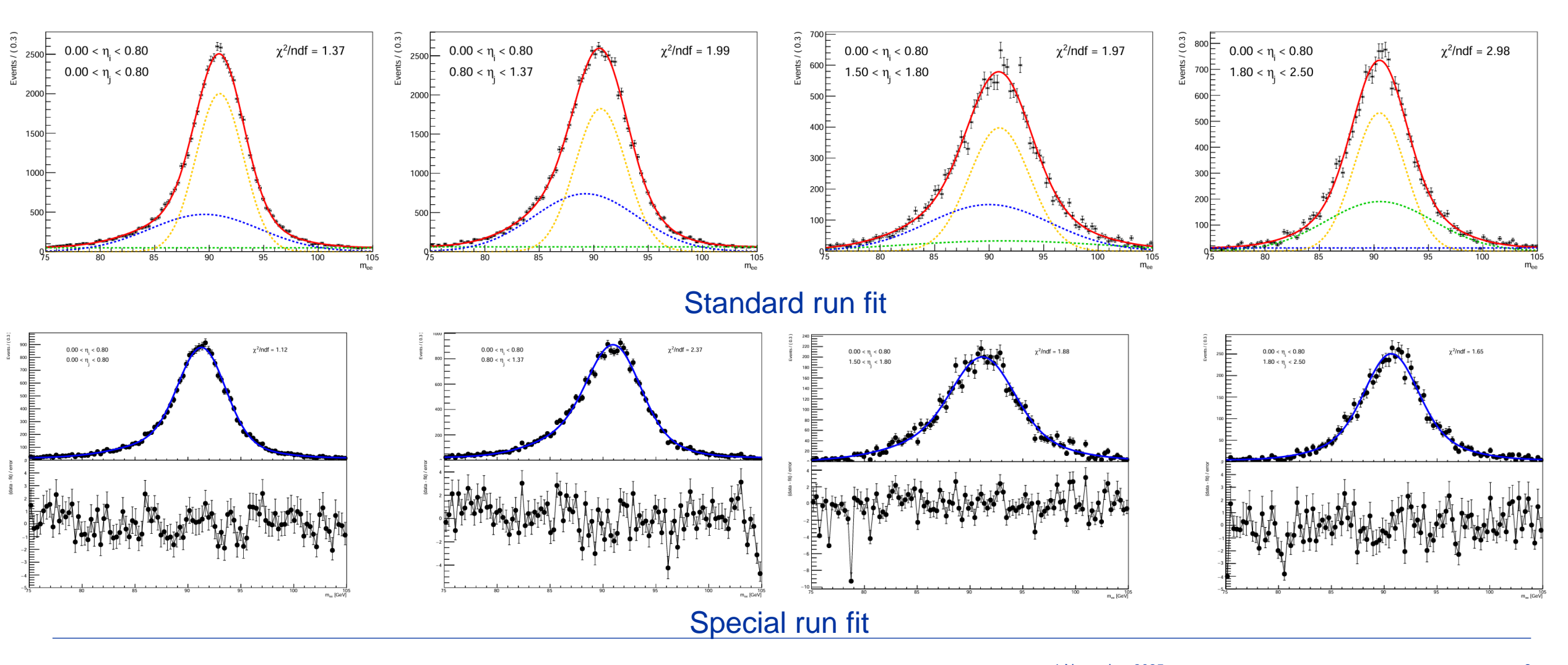
$$\mu_{special} = \mu_{std} \cdot \sqrt{(1 + \alpha_i)(1 + \alpha_j)}$$

$$\sigma_{special} = \sqrt{(1 + \alpha_i)(1 + \alpha_j)} \cdot \sigma_{std}$$
where i and j are  $|\eta|$  regions

 $\triangleright$  Fit all of the  $m_{ee}$  histograms of special run to obtain  $\alpha$ 

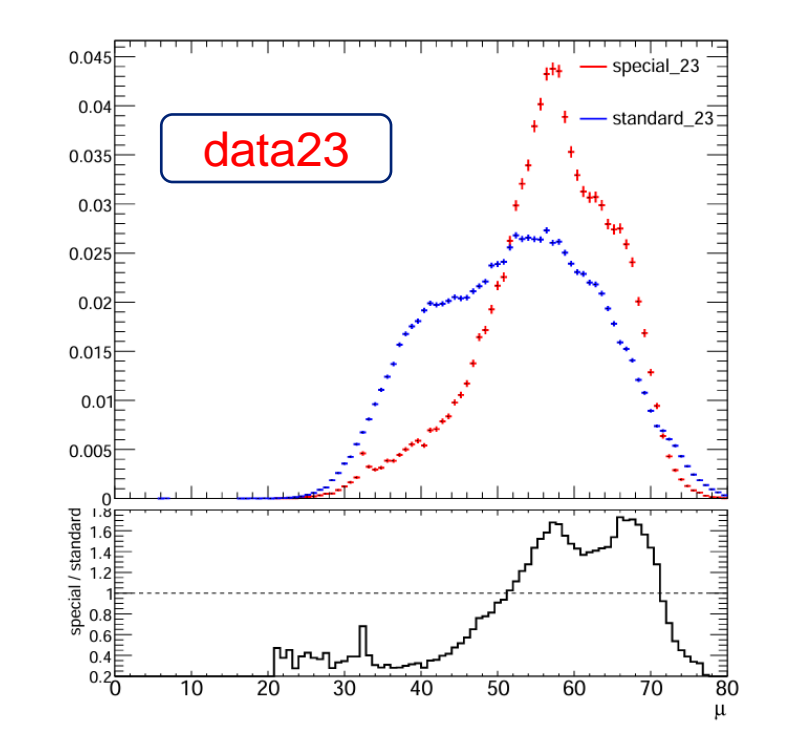
# M<sub>ee</sub> fit results

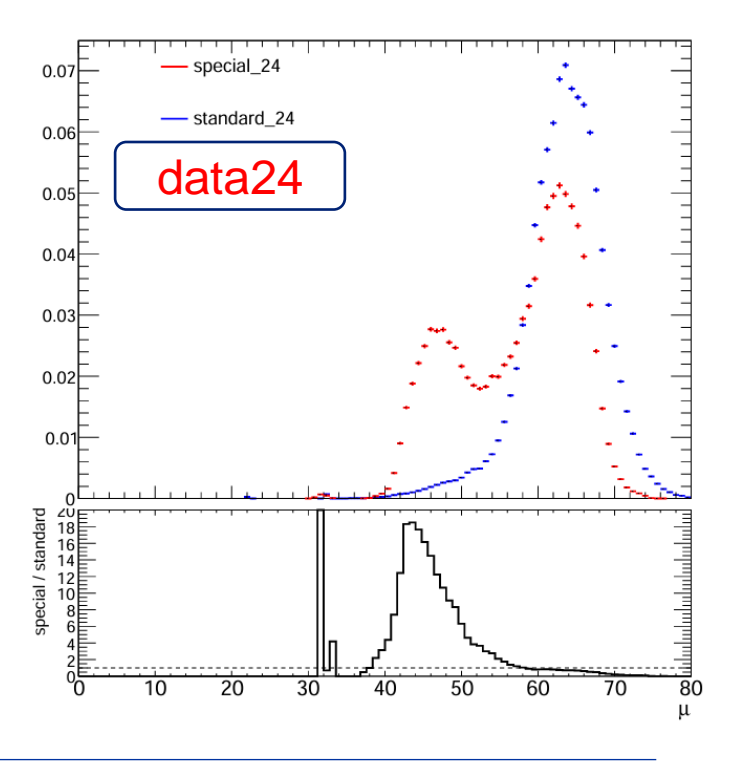
• Standard and special runs  $m_{ee}$  fits in some  $|\eta|$  regions



## Pile-up dependency studies

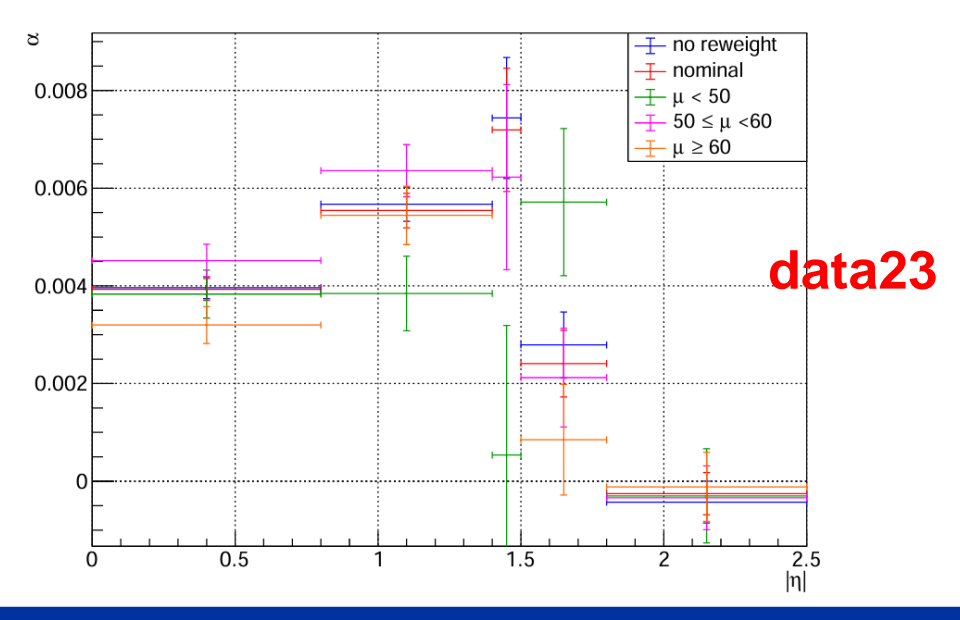
- After event selection, the pile-up distribution of the standard and special runs look very different.
- In order to match the special run, the events in standard run are reweighted (nominal case).
- To study the pile-up dependency, the pile-up inclusive region is divided into three regions and the results in individual region can be obtained
  - ➤ Data23
    - $\mu < 50$
    - $50 \le \mu < 60$
    - $\mu \ge 60$
  - ➤ Data24
    - $\mu < 58$
    - $58 \le \mu < 64$
    - $\mu \ge 64$





#### Results of data23 and data24

- The impact of pile-up is not huge both in data23 and data24 especially in the first region.
- The difference of two results are mainly come from 1<sup>st</sup>, 3<sup>rd</sup> and 5<sup>th</sup> region about 0.1%.



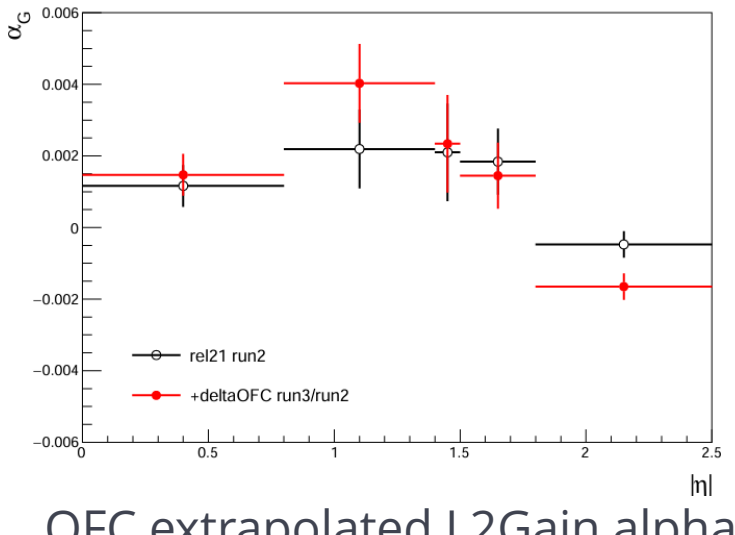
ර 0.006			$T$ no reweight $T$ nominal $T$ $\mu$ < 58 $T$ 58 $\leq$ $\mu$ < 64
0.005		1	1 μ ≥ 64
0.004		- <del> </del>	
0.003		<u> </u>	data24
0.002	<u> </u>		
0.001	=		
0	<u> </u>	1	
(	0.5	1 1.5	2 2.5  n

$ \eta $	[0, 0.8)	[0.8, 1.37)	[1.37, 1.5)	[1.5, 1.8)	[1.8, 2.47]
Without reweight	$3.96 \pm 0.22$	$5.67 \pm 0.35$	$7.44 \pm 1.24$	$2.79 \pm 0.68$	$-0.43 \pm 0.43$
nominal	$3.93 \pm 0.22$	$5.54 \pm 0.35$	$7.19 \pm 1.26$	$2.41 \pm 0.68$	$-0.25 \pm 0.43$
$\mu < 50$	$3.83 \pm 0.49$	$3.84 \pm 0.76$	$5.37 \pm 2.66$	$5.71 \pm 1.51$	$-0.30 \pm 0.97$
$50 \le \mu < 60$	$4.52 \pm 0.36$	$6.36 \pm 0.53$	$6.22 \pm 1.90$	$2.12 \pm 1.01$	$-0.34 \pm 0.66$
$\mu \ge 60$	$3.20 \pm 0.38$	$5.44 \pm 0.60$	$11.8 \pm 2.06$	$0.85 \pm 1.13$	$-0.11 \pm 0.71$

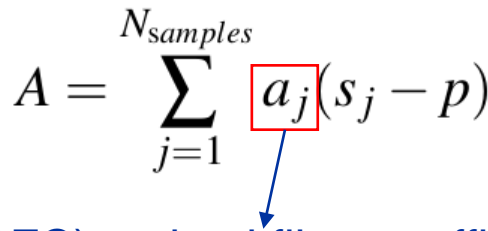
$ oldsymbol{\eta} $	[0, 0.8)	[0.8, 1.37)	[1.37, 1.5)	[1.5, 1.8)	[1.8, 2.47]
Without reweight	$2.80 \pm 0.16$	$4.96 \pm 0.25$	$5.48 \pm 0.89$	$0.70 \pm 0.47$	$-0.22 \pm 0.31$
nominal	$3.01 \pm 0.16$	$5.44 \pm 0.25$	$4.45 \pm 0.85$	$2.36 \pm 0.46$	$-1.13 \pm 0.30$
$\mu < 58$	$2.99 \pm 0.23$	$5.34 \pm 0.37$	$2.85 \pm 1.25$	$2.94 \pm 0.65$	$-1.03 \pm 0.44$
$58 \le \mu < 64$	$3.09 \pm 0.28$	$5.03 \pm 0.45$	$3.90 \pm 1.57$	$1.55 \pm 0.82$	$-1.27 \pm 0.53$
$\mu \geq 64$	$2.95 \pm 0.33$	$5.87 \pm 0.54$	$5.63 \pm 1.92$	$1.99 \pm 0.99$	$-0.68 \pm 0.65$

#### Difference between Run3 and extrapolated results

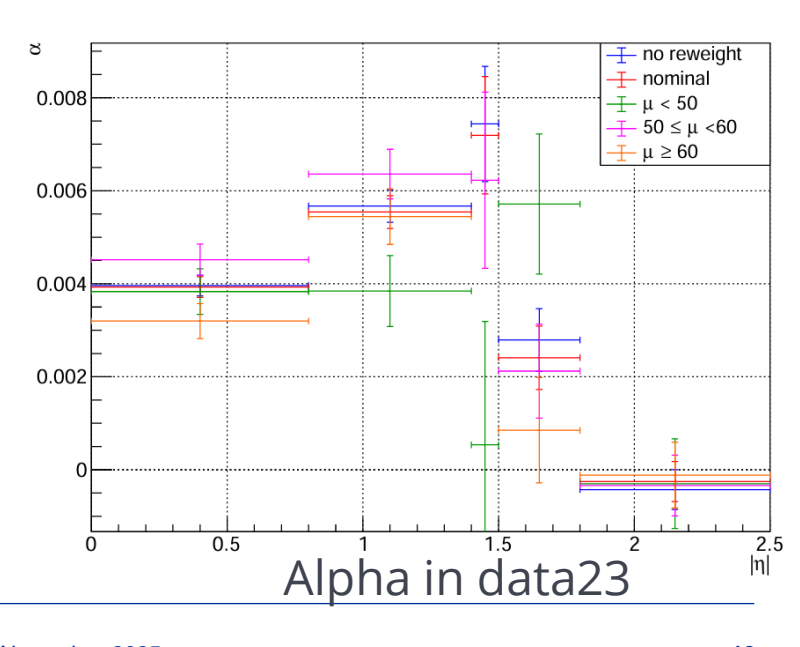
- The red points are our expected results considering the OFC difference between Run2 and Run3
  - Current run3 results in data23 have about +0.2% shift
- The main reason of the shift is the difference of FEB configurations in special runs
  - For Run2 special run, only the thresholds of Layer 2 HG/MG are changed
  - For Run3 special run, both of the thresholds of Layer1 and Layer2 HG/MG are changed
- The results of Run2 just consider the effect of L2, but current results consider the combined effect of L1 and L2
  - That the results are higher than extrapolated results is reasonable



OFC extrapolated L2Gain alpha



(OFC) optimal filter coefficients



## **Energy deposition in per layer**

•  $|\eta|$  region considered:  $|\eta| < 0.8$ 

<b>E0</b>	Standard Run		Special Run		Rel. difference	
	leading	subleading	leading	subleading	leading	subleading
Data18	1.840	1.649	1.841	1.636	0.05%	-0.79%
Data23	1.828	1.629	1.835	1.624	0.38%	-0.31%

$\mathbf{E0}$	Standard Run		Special Run		Rel. difference	
	leading	subleading	leading	subleading	leading	subleading
Data18	1.840	1.649	1.841	1.636	0.05%	-0.79%
Data23	1.828	1.629	1.835	1.624	0.38%	-0.31%
	I .		I .		I.	

The	unit is	s Ge	V in	the	tabl	les
1110	uiiit i		A 111	uic	luoi	

> Rel. differences are calculated by

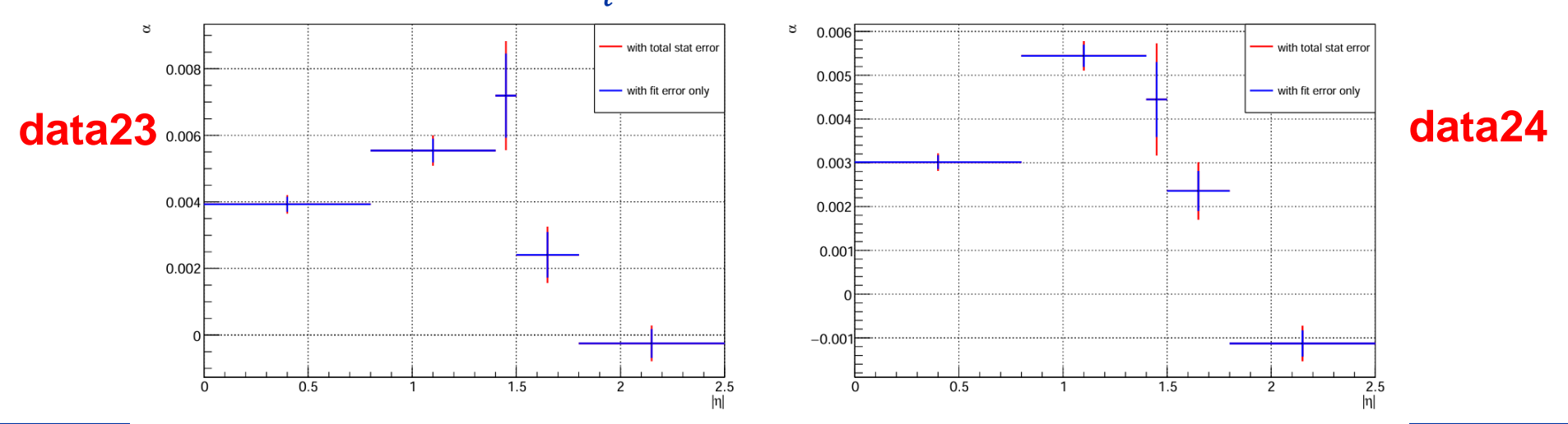
$\mu_{special} - \mu_{standard}$	$\sigma_{special} - \sigma_{standard}$
$\mu_{standard}$ ,	$\sigma_{standard}$

<b>E2</b>	Standard Run		Special Run		Rel. difference	
	leading	subleading	leading	subleading	leading	subleading
Data18	32.735	24.997	32.945	25.248	0.64%	1.00%
Data23	32.849	25.125	33.157	25.290	0.94%	0.66%

The E1 difference between special and standard runs are bigger in data23 since the threshold is changed.

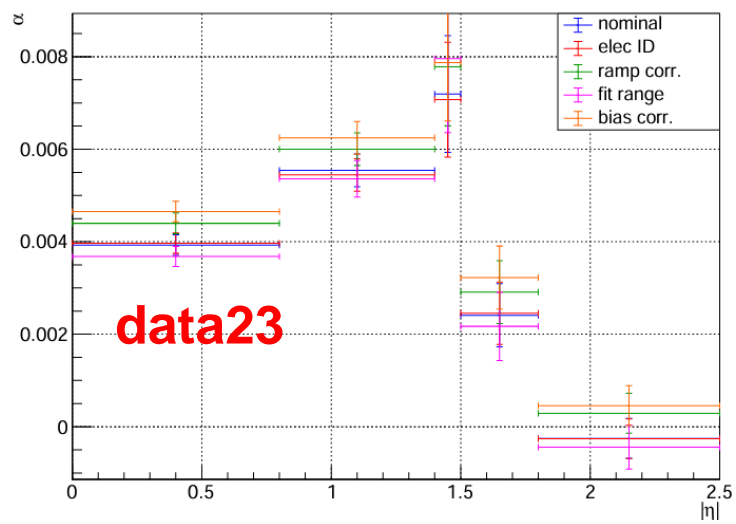
#### **Statistical uncertainty**

- The statistical uncertainties consist of two parts
  - > Special run statistic
    - Reflected in the uncertainties of special run fit results
  - > Standard run statistic
    - Propagated to the value of the extracted  $\alpha_i$  through bootstrapping
    - Generate 100 replicas with a Poisson weight distribution ( $\lambda = 1$ ) to obtain the distribution of  $\alpha_i$
    - The uncertainties are the std dev of  $\alpha_i$  distribution



## **Systematic uncertainties**

- The systematic uncertainties mainly come from four sources
  - **Electron ID**: both electron candidates pass the loose likelihood ID instead of the medium ID
  - > Ramp correction: "average" ramp correction is applied to the cell energy in L2 instead of "cell-by-cell" correction
  - Fit range: set the fit range of  $m_{e^+e^-}$  as [85, 95]GeV instead of [75, 105]GeV
  - **Bias correction**: the bias correction (from calibration board offset) is applied instead of no correction



		<u> </u>			1
		0	0.5 1	1.5	2 2.5  η
η	statistical uncertainty	Elec ID (syst.)	Ramp corr. (syst.)	Fit range (syst.)	Bias corr. (syst.)
[0, 0.8)	0.22	0.07	0.47	0.25	0.72
[0.8, 1.37)	0.35	0.09	0.46	0.18	0.71
[1.37, 1.5)	1.26	0.12	0.59	0.77	0.68
[1.5, 1.8)	0.68	0.04	0.50	0.24	0.82
[1.8, 2.47]	0.43	0.01	0.04	0.19	0.71

യ.006	T nominal
۵.000	
	- lec ID
0.005	T ramp corr.
0.003	fit range
	- I his som
0.004	bias corr.
0.004	
0.003	
0.002	<u> </u>
0.001	
	data24
	- Gatal I
0	
·	
-0.001	
-0.001	
	0.5 1 1.5 2 2.5
,	0.5 1 1.5 2 2.5  m
	ļΨ.

	$\eta$	statistical uncertainty	Elec ID (syst.)	Ramp corr. (syst.)	Fit range (syst.)	Bias corr. (syst.)
	[0, 0.8)	0.16	0.02	0.53	0.26	0.75
	[0.8, 1.37)	0.25	0.13	0.45	1.61	0.64
	[1.37, 1.5)	0.85	0.21	0.42	0.33	0.64
	[1.5, 1.8)	0.45	0.03	0.38	0.84	0.62
-[	[1.8, 2.47]	0.30	0.01	0.50	0.27	0.64

#### **Summary**

- The L2 HG/MG intercalibration measurement using Run3 datasets(23 and 24) has been presented:
  - ➤ There is a positive shift when comparing with previous Run2 results
- Differences in the special run configuration settings account for the discrepancy between the data18 and data23 measurements
  - ➤ The results of data18 only consider the effect of L2 HG/MG
  - > while the results of data23 consider the combined effect of L1 and L2

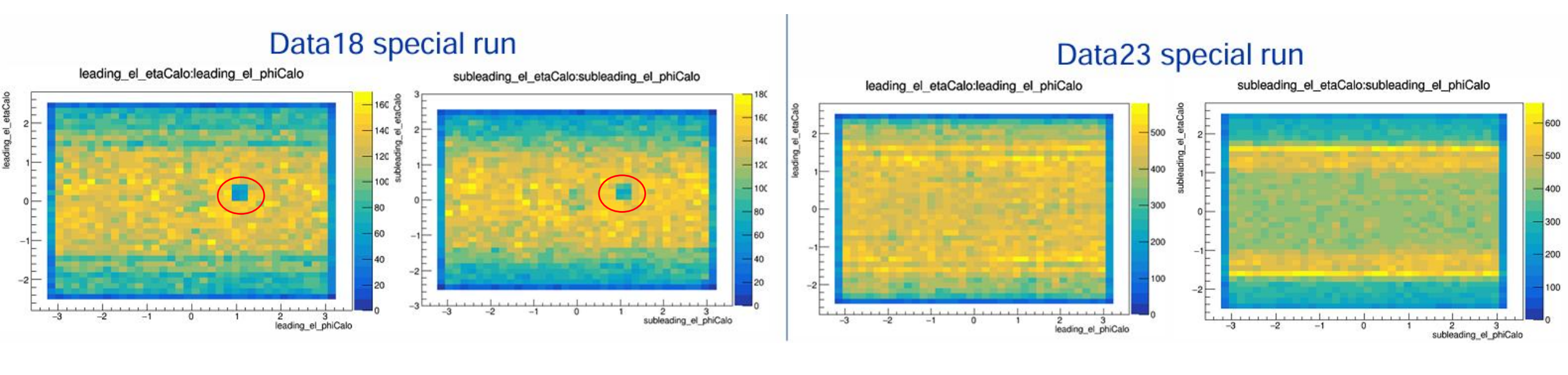
#### Outlook

- > the study of ADC non-linearity correction with Run3 samples in L1
- ➤ Apply L1 and L2 HG/MG correction and update the results
- ➤ Only L2 HG/MG thresholds were lowered in data25, enabling comparison with data23/data24

# Back up

# Run2 special run issue

• The issue is fixed in run3



## L1 configurations for standard and special run

Thu May 416:31:39 2023 UTC - Sat May 6 09:03:39 2023 UTC (956366848) [ID (UInt32) : 956366848], [Name (String255) : barrel A 01L F1], [upper1 (Int32) : 3600], [upper2 (Int32) : 3600], [upper5 (Int32) : 3600], [upper5 (Int32) : 3600],

lower10 (lnt32): 1045], [lower11 (lnt32): 1063], [lower12 (lnt32): 1038], [lower13 (lnt32): 1052], [lower14 (lnt32): 1037], [lower15 (lnt32): 1044], [lower16 (lnt32): 1019], [lower17 (lnt32): 1080], [lower18 (lnt32): 1073], [lower19 (lnt32): 1078], [lower20 (lnt32): 1053], [lower21 (lnt32): 1069], [lower22 (lnt32): 1071], [lower23 (lnt32): 1105], [lower24 (lnt32): 1055], [lower25 (lnt32): 1071], [lower26 (lnt32): 1078], [lower27 (lnt32): 1099], [lower28 (lnt32): 1075], [lower29 (lnt32): 1087], [lower30 (lnt32): 1099], [lower31 [lnt32): 1101], [lower32 (lnt32): 1084], [lower33 (lnt32): 1090], [lower34 (lnt32): 1095], [lower35 (lnt32): 1090], [lower36 (lnt32): 1078], [lower37 (lnt32): 1097], [lower48 (lnt32): 1097], [lower40 (lnt32): 11081], [lower41 (lnt32): 1117], [lower42 (lnt32): 1107], [lower42 (lnt32): 1107], [lower48 (lnt32): 1108], [lower48 (lnt32): 1107], [lower49 (lnt32): 1108], [lower48 (lnt32): 1101], [lower50 (lnt32): 1100], [lower50 (lnt32): 1100], [lower50 (lnt32): 1108], [lower62 (lnt32): 1098], [lower62 (lnt32): 1094], [lower63 (lnt32): 1097], [lower64 (lnt32): 1091], [lower65 (lnt32): 1097], [lower66 (lnt32): 1099], [lower67 (lnt32): 1088], [lower68 (lnt32): 1089], [lower68 (lnt32): 1097], [lower67 (lnt32): 1088], [lower68 (lnt32): 1089], [lower68 (lnt32): 1099], [lower68 (lnt32): 1099], [lower68 (lnt32): 1099], [lower68 (lnt32): 1088], [lower68 (lnt32): 1089], [lower68 (lnt32): 1099], [lower68 (lnt32): 1088], [lower68 (lnt32): 1088], [lower68 (lnt32): 1088], [lower68 (lnt32): 1099], [lower68 (lnt32): 1099], [lower68 (lnt32): 1088], [lower68 (lnt32): 1088], [lower68 (lnt32): 1099], [lower68 (lnt32): 109

at May 6 09:03:39 2023 UTC - Sat May 27 13:35:19 2023 UTC (956366848) [ID (UInt32) : 956366848], [Name (String255) : barrel A 01L F1], [upper1 (Int32) : 3600], [upper2 (Int32) : 3600], [upper5 (Int32) : 3600],

[lower26 (Int32): 1277], [lower37 (Int32): 1285], [lower38 (Int32): 1270], [lower29 (Int32): 1289], [lower30 (Int32): 1310], [lower31 (Int32): 1285], [lower32 (Int32): 1280], [lower33 (Int32): 1275], [lower34 (Int32): 1280], [lower35 (Int32): 1289], [lower36 (Int32): 1283], [lower37 (Int32): 1297], [lower38 (Int32): 1283], [lower39 (Int32): 1282], [lower40 (Int32): 1298], [lower41 (Int32): 1313], [lower42 (Int32): 1306], [lower43 (Int32): 1306], [lower44 (Int32): 1297], [lower45 (Int32): 1312], [lower46 (Int32): 1302], [lower47 (Int32): 1306], [lower48 (Int32): 1306], [lower49 (Int32): 1290], [lower50 (Int32): 1290], [lower51 (Int32): 1301], [lower52 (Int32): 1296], [lower53 (Int32): 1294], [lower54 (Int32): 1305], [lower55 (Int32): 1308], [lower56 (Int32): 1298], [lower57 (Int32): 1290], [lower58 (Int32): 1291], [lower64 (Int32): 1292], [lower65 (Int32): 1265], [lower66 (Int32): 1286], [lower67 (Int32): 1286], [lower68 (Int32): 1269], [lower69 (Int32): 1285], [lower70 (Int32): 1287], [lower71 (Int32): 1277], [lower72 (Int32): 1282], [lower73 (Int32): 1269],

Setting for special run: ADC counts ~ 1000

Setting for standard run: ADC counts ~ 1300

## **Trigger in Run3**

- Trigger in Run3 datasets
  - ➤ Data23 special run: HLT\_2e24\_lhvloose\_L12EM20VH
  - ➤ Data23 standard run and data24: both of HLT\_2e24\_lhvloose\_L12EM20VH and HLT\_2e24\_lhvloose\_L12eEM24L
  - ➤In the talk, only HLT\_2e24\_lhvloose\_L12EM20VH is considered for data23

#### The energy response difference between HG and MG

$$\geq \frac{\Delta E}{E} = \alpha_G(\eta) \cdot \frac{1}{\delta_Z(\eta)} \cdot \delta_{MG}^{e,\gamma}(\eta, E_T)$$

- $\triangleright \alpha_G(\eta)$  is the energy scale difference
- $\delta_Z(\eta)$  quantifies the fractional change in energy for electrons from Z-boson decays between the data with lower and standard thresholds for a given change in the energy recorded in MG. This sensitivity factor is about 0.3 to 0.4 (0.2 to 0.25) in the barrel (endcap) calorimeter. It takes into account the fact that only a fraction of the electron energy is recorded in MG in the special-settings data taking, while in data recorded with normal settings some cells in the second layer can be read out in MG. This is particularly true for the endcaps, where the electron energies are larger.
- $\delta_{\text{MG}}^{e,\gamma}(\eta, E_{\text{T}})$  quantifies, for a given particle, the fractional change in total energy for a given change in the energy recorded in MG, for standard gain thresholds. It is estimated using simulated single-particle samples. It is close to zero up to  $E_{\text{T}} = 50 \,\text{GeV}$  for electrons and  $E_{\text{T}} = 40 \,\text{GeV}$  for photons, and rises to reach a maximum value of about 0.7 for  $E_{\text{T}} \sim 400 \,\text{GeV}$  in the barrel, and of about 0.5 for  $E_{\text{T}} \sim 200 \,\text{GeV}$  in the endcap. Above these values,  $\delta_{\text{MG}}^{e,\gamma}(\eta, E_{\text{T}})$  decreases as the low-gain readout starts contributing.

#### **ΔE** difference

- •In correction files
  - ➤ for MG the correction energies are almost lower than 0
  - ➤ but for HG the correction energies are almost higher than 0
- Look at the MG purity for leading and subleading electrons, subleading electrons have less MG cells
- Therefore, the correction energies of subleading electrons are higher than leading electrons

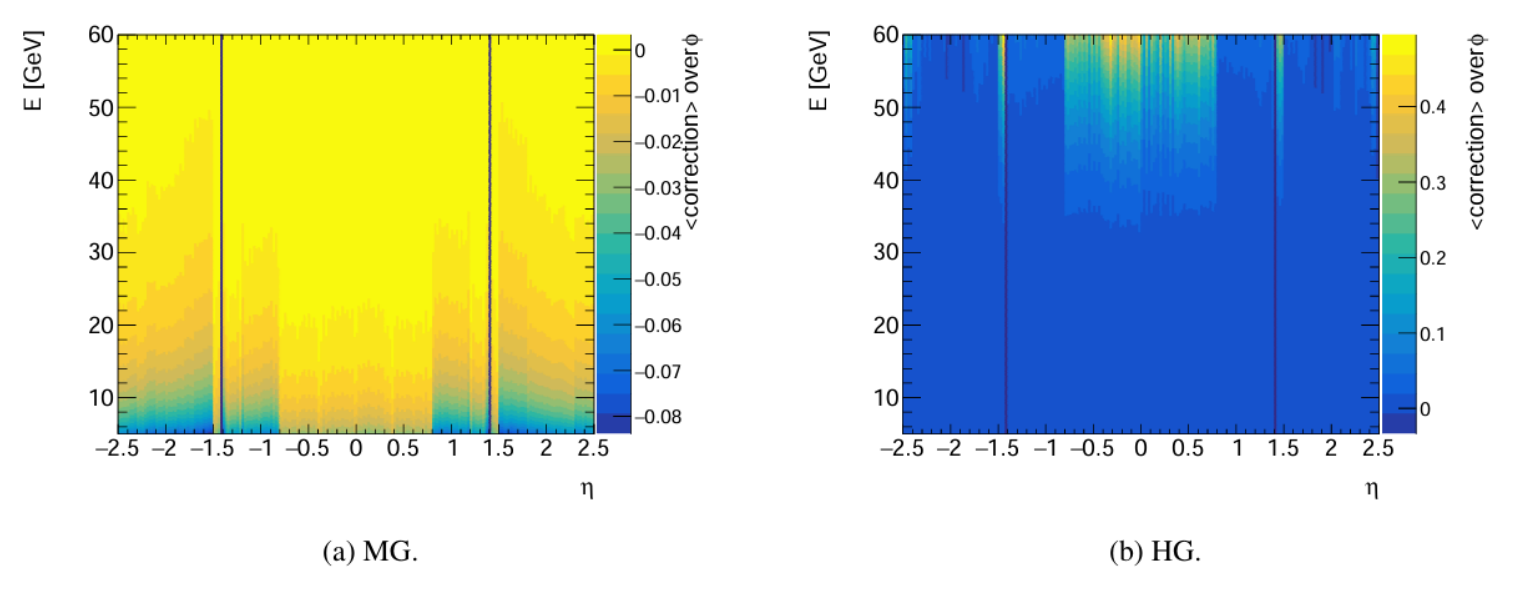


Figure 49: Map of the correction in the  $E - \eta$  space of the second layer of the LAr calorimeter.

